Journal of Biomedical Optics

SPIEDigitalLibrary.org/jbo

Red-luminescent europium (III) doped silica nanoshells: synthesis, characterization, and their interaction with HeLa cells

Jian Yang
Sergio Sandoval
Jesus G. Alfaro
Sharraya Aschemeyer
Alex Liberman
David T. Martin
Milan Makale
Andrew C. Kummel
William C. Trogler

SPIE

Red-luminescent europium (III) doped silica nanoshells: synthesis, characterization, and their interaction with HeLa cells

Jian Yang,[a] Sergio Sandoval,[b] Jesus G. Alfaro,[c] Sharraya Aschemeyer,[a] Alex Liberman,[b] David T. Martin,[d] Milan Makale,[e] Andrew C. Kummel,[a] and William C. Trogler[a]
[a]University of California, San Diego, Department of Chemistry and Biochemistry, 9500 Gilman Drive, La Jolla, California 92093
[b]University of California, San Diego, Department of Bioengineering, 9500 Gilman Drive, La Jolla, California 92093
[c]University of California, San Diego, Department of Chemical Engineering, 9500 Gilman Drive, La Jolla, California 92093
[d]University of California, San Diego, Department of Computer and Electrical Engineering, 9500 Gilman Drive, La Jolla, California 92093
[e]University of California, San Diego, Moores Cancer Center, 9500 Gilman Drive, La Jolla, California 92093

Abstract. A simple method to fabricate Eu^{3+} doped silica nanoshells particles with 100 and 200 nm diameters is reported. Amino polystyrene beads were used as templates, and an 8 to 10 nm thick silica gel coating was formed by the sol-gel reaction. After removing the template by calcination, porous dehydrated silica gel nanoshells of uniform size were obtained. The Eu^{3+} doped silica nanoshells exhibited a red emission at 615 nm on UV excitation. The porous structure of the silica shell wall was characterized by transmission electron microscopy measurements, while particle size and zeta potentials of the particles suspended in aqueous solution were characterized by dynamic light scattering. Two-photon microscopy was used to image the nanoshells after assimilation by HeLa cancer cells. © *2011 Society of Photo-Optical Instrumentation Engineers (SPIE).* [DOI: 10.1117/1.3593003]

Keywords: europium; silica; luminescent; nanoshells; endocytosis.

Paper 10563R received Oct. 18, 2010; revised manuscript received Apr. 20, 2010; accepted for publication Apr. 26, 2011; published online Jun. 14, 2011.

1 Introduction

An important area of biomedical nanotechnology is based on the interaction of living systems with inorganic and organic materials at the nanoscale. Silica nanoparticles (NPs) are attractive biomaterials because of their advantages as readily functionalized transport and imaging devices:[1–3] silica has low cellular biotoxicity and good biocompatibility,[4] the surface of silica can be modified readily with trimethoxysilyl reagents[5,6] that allows for easy surface modification such as for attaching biomolecules,[5,7] and silica can be used to encapsulate small molecules.[8] Silica NPs potentially have multiple biomedical applications as imaging agents, targeted drug delivery agents, or gene transferring motherships.[9–12]

Fluorescent silica NPs have been used for imaging in cell culture and animal *in vivo* studies.[13,14] The organic fluorescent dyes used are either covalently conjugated to the surface of silica[15] or encapsulated in the SiO_2 core.[16] Organic dyes are limited by their broad emission range, photobleaching, short fluorescence lifetimes, and high cost. Furthermore, functionalization of the silica surface with dye molecules reduces the reactive surface sites available for coupling targeting agents to the NPs. Other groups have synthesized silica NPs with different inorganic luminescent quantum dot (QD) sources;[17–19] however, these NPs do not have a viable future in human *in vivo* studies due to the toxicity of the QD components. Rare-earth ions such as Eu^{3+}, Er^{3+}, or Y^{3+} doped into insulators often yield efficient inorganic luminescent centers. Rare-earth ions have narrow emission spectral peaks and long emission lifetimes, and they are believed to be noncytotoxic.[20] We previously reported a simple method of synthesis of silica and titania nanoshell (NS) particles with amino polystyrene (APS) beads as templates.[21] In this manuscript, a method for preparing Eu^{3+} doped silica NS is reported. The uniqueness of these NS particles lies in the fact that the fluorophore reporter is directly incorporated in the NS matrix, leaving the entire NS surface free for future targeting or biomolecule fictionalization while also leaving the NS core free for drug or biomolecule encapsulation. Hydrolyzed tetramethyl orthosilicate (TMOS) was used as a precursor of silica. APS beads were used as templates in the sol-gel reaction, and $Eu(NO_3)_3$ was added as the dopant. The reaction employed ethanol solvent at room temperature, and the APS cores were removed by calcination. The size of NS could be controlled by using APS beads with different diameters. The NS had uniform and robust silica walls of 8 to 10 nm thickness with Eu(III) doping levels below 3% mole fraction. When the Eu^{3+} content exceeded 3%, only irregularly sized colloidal material was obtained. The Eu^{3+} doped silica NS showed a narrow emission at 615 nm under UV excitation. This provides a simple, inexpensive, and scalable method to prepare Eu^{3+} doped silica NS for imaging studies. The long-lived atomic emission of Eu(III) makes it an efficient two-photon absorber. This manuscript also

Address all correspondence to: William C. Trogler, University of California San Diego, Chemistry and Biochemistry, 9500 Gilman Drive – Mail Code 0358, La Jolla, CA 92093-0358. Tel: 858-534-6175; Fax: 858-534-5383; E-mail: wtrogler@ucsd.edu.

1083-3668/2011/16(6)/066012/8/$25.00 © 2011 SPIE

reports on the interaction of these luminescent silica spheres with HeLa cancer cells as probed by two-photon spectroscopy.

2 Experimental Methods and Materials

2.1 *Materials*

Tetramethyl orthosilicate and europium nitrate hydrate were obtained from Aldrich-Sigma Ltd. All chemicals were used as received. The 100-nm amine functionalized polystyrene beads (2.5% w/w) were purchased from PolySciences Ltd. Nunc Lab-Tek II 4-well chamber slides were obtained from Fisher Scientific (Pittsburgh, Pennsylvania). HeLa cervical cancer cells were purchased from ATCC (Manassas, Virginia); Dulbecco's Phosphate Buffer Saline solution (DPBS 1×), Dulbecco's Modified Eagle's Medium (DMEM), and fetal bovine serum (FBS) were purchased from Mediatech, Inc. Manassas, Virginia); while media supplements, Chloromethylfluorescein Diacetate (CMFDA) CellTracker^{TM} Green intracellular stain and Prolong Gold were obtained from Invitrogen (Carlsbad, California). Paraformaldehyde (PFA) was purchased from ThermoFisher Scientific (Fair Lawn, New Jersey).

2.2 *Preparation of Europium Doped Silica Nanoshells*

In a 2 mL Eppendorf tube, 100 uL of a 2.5% weight dispersion (in water) of 100 nm APS beads were suspended in 1.75 mL of absolute ethanol. To this suspension, 6.5 uL of TMOS and then 250 uL of 1 mg/mL $Eu(NO_3)_3 \cdot 5H_2O$/ethanol was added. The mixture was stirred on a vortex mixer at room temperature at a speed of 900 rpm. After 12 h of stirring, a white precipitate was collected by centrifugation and washed with ethanol and dried in vacuum for 48 h at room temperature to give 4.1 mg of core-shell spheres.

The APS core was removed by calcining the 4.1 mg of core-shell nanospheres by heating in air at 5°C per min to 500°C and maintaining this temperature for 24 h. About 1.5 mg of europium doped SiO_2 nanoshells were collected as a white powder. Energy dispersive X-ray spectroscopy (EDS) showed the Eu content of this preparation was 1.35% (mole%).

To increase the absorption efficiency of Eu/SiO_2 nanoshells by HeLa cells, poly(ethylenimine) (PEI) was coated on the spheres, thereby increasing the positive charge of the surface that was hypothesized to improve adherence to the negatively charged HeLa cells. The following coating procedure was employed: 3 mg of Eu-SiO_2 nanoshells were suspended in 1.5 mL of 0.1mg/mL PEI water solution. The suspension was stirred for 2 hours and the NS were collected by centrifugation and washed with water. Afterward, the PEI coated NS were suspended in 0.5 mL of pH 7.4 phosphate buffer for the cell experiments.

2.3 *Characterization of Silica Nanoshells*

The scanning electron microscopy (SEM) and EDS measurements were conducted on an FEI/Philips XL30 FEG ESEM microscope with an accelerating voltage of 10 kV. The average diameter of the nanospheres was determined from SEM images. Transmission electron microscopy (TEM) images were obtained with the use of a JEOL-2000EX (200 kV) CryoElectro microscope with an accelerating voltage of 200 kV. A Perkin-Elmer LS 45 luminescence spectrometer was used to record emission and excitation spectra. A Zetasizer Nano ZS from Malvern Instruments was used to determine the dynamic light scattering (DLS) size distributions and zeta potentials of nanoshells when resuspended in distilled water with gentle sonication.

2.4 *Cell Culture*

HeLa cervical cancer cells were grown at 5×10^4 cells/well on Nunc Lab-Tek II 4-well chamber slides in DMEM supplemented with 10% FBS, 1% antibiotics (Penicillin, Streptomycin, Glutamine), and 1% sodium pyruvate, at 37°C in a humidified atmosphere of 5% CO_2. Before starting cell adhesion/endocytosing experiments, the cells were grown to 60 to 80% well confluency.

2.5 *Cell Adhesion/Endocytosis Experiments*

In order to determine the extent of NS cell adhesion/endocytosis, HeLa cells were incubated with 500 μg/mL of europium SiO_2 NS functionalized with amines for 24 h in DMEM complete media at 37°C in a humidified atmosphere of 5% CO_2. Afterward, cells were washed twice with DPBS and labeled with 2.5 μM CMFDA CellTracker Green intracellular stain in DPBS for 30 min. Subsequently, cells were washed 3× with DPBS to remove any excess dye, fixed with 4% PFA in DPBS solution, washed twice more with DPBS, and covered with Prolong Gold antifade reagent in order to prepare samples for visualization by two-photon microscopy.

2.6 *Two-Photon Microscopy of Silica Nanoshells Engaging HeLa Cells In Vitro*

Two-photon (2-P) fluorescence dual color (red/green europium SiO_2 NS/CMFDA) images were obtained with a custom modified Nikon FN1 intravital microscope fitted with a 60× water immersion objective (Nikon, 1.2 NA). The instrument was driven by a Spectraphysics MaiTai Ti:Sa 3 Watt, 120 femtosecond pulsed laser tuned to 695 nm. The microscope operated in non-descanned mode. Emitted sample light was separated into red/green channels using a beam splitter and band pass filters (Chroma ET620/60 and ET510/50). Two side-on PMTS (Hamamatsu) captured the light, and the raster scan data was assembled and saved using Nikon EZ-1 display/analysis software. Images were initially acquired full field at 60×, with constant gain settings between samples, and regions of interest (ROIs) were magnified 4× by spatially compressing the raster scan. In order to confirm the location of the nanospheres, image volumes composed of multiple 1-μm XY slices were serially acquired along the sample z-axis. 2-P images were further processed for background level and SNR, using Image J (NIH, Bethesda, Maryland) and custom C#-based software written in-house.

3 Results and Discussion

3.1 *Synthesis of Eu-SiO_2 Nanoshells*

The synthesis of APS/Eu-SiO_2 core-shell spheres used absolute ethanol as a solvent to slow the sol-gel process. Previously, the fabrication of SiO_2 shells on APS beads with the assistance of poly-L-lysine in pH 7.4 PBS buffer was reported.[21] The hydrolyzed intermediate of TMOS, silicic acid, was used as

Table 1 Content of europium (III) in silica nanoshells.

100-nm APS beads template		200-nm APS beads template	
Initial content of Eu^{3+} to TMOS (%mole)	Eu^{3+} content in nanoshells (%mole)[a]	Initial content of Eu^{3+} to TMOS (%mole)	Eu^{3+} content in nanoshells (%mole)[a]
0.10	0.11	0.05	0.04
0.23	0.45	0.10	0.06
0.46	1.35	0.23	0.54
0.70	2.84	0.46	1.02

[a]From EDS analysis, compared to Si and O.

the precursor of the SiO_2 layer. To dope Eu^{3+} into the SiO_2 matrix, the procedure was modified to decrease the rate of formation of the silica shell. TMOS instead of silicic acid was used as a precursor of SiO_2, and absolute ethanol instead of PBS was employed as a solvent for the hydrolysis of TMOS and the cross-linking of SiO^{4-}. The slowing of the kinetics was crucial in incorporating Eu^{3+} in the NS wall and creating uniform Eu-SiO_2 NS as the presence of $Eu(NO_3)_3$ tended to encourage the formation of colloidal SiO_2 when PBS buffer was used during the sol-gel reaction. The small amount of water for the hydrolysis reaction in this mixture (5% by volume) arises from the added aqueous APS suspension. Formation of the Eu-SiO_2 shell required 12 h of reaction time compared with only 5 min for the formation of the SiO_2 layer in aqueous PBS buffer. The partially protonated amine groups on the surface of APS beads help attract the negative silicic acid precursor to the surface of beads and concurrently Eu^{3+} was trapped into the silica matrix perhaps aided by the ligating amino groups.

Both 100- and 200-nm APS beads were used as templates and variable amounts of Eu^{3+} were doped into the silica NS. Table 1 shows the concentration of $Eu(NO_3)_3$ used in the reaction and the content of atomic europium obtained in the NS. The results depict a general trend where as more $Eu(NO_3)_3$ is added in the initial reaction, more atomic europium is incorporated in the NS wall matrix, with a higher europium %mole being entrapped in the NS wall lining than what was used in the original solution, signifying that not all of the TMOS used reacts during the sol-gel process. In addition, it was observed that if the content of europium is too high, broken silica shells and small pieces of colloids occurred at a higher frequency and were visible in SEM images. The radius of Eu^{3+} is 1.087 Å, which is much larger than the radius of Si^{4+} (0.41 Å), consequently, a high concentration of Eu^{3+} in the silica matrix or on the surface of the APS beads could hinder formation of a uniform silica shell and could account for the colloids and broken shells.

The APS core was removed by calcination from core-shell spheres at 500°C for 24 h. Figure 1 shows SEM images of Eu-SiO_2 spheres prepared using 100- and 200-nm APS beads after calcination and a TEM image of the 200 nm Eu-SiO_2 shells. Microscopy images confirmed the hollow shell morphology and revealed that the thickness of the Eu-SiO_2 shell wall was 8 to 10 nm. According to the SEM pictures, the diameters of the nanoshells are 87 ± 9 and 179 ± 15 nm for 100 and 200 nm hollow shells. The shell size shrank below that of the APS template during calcination; it is hypothesized that calcination dehydrates the silica, initially forming a silica gel coating around the APS template, which results in the contracted size for the NS. The shrinkage of a gel is a common occurrence as

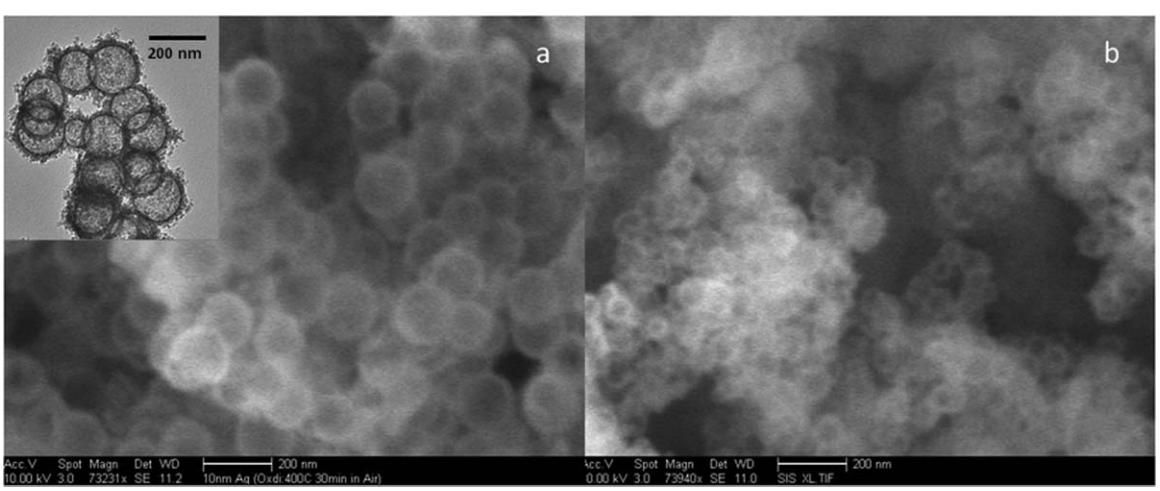

Fig. 1 SEM and TEM images of europium doped silica nanoshells from (a) 200 and (b) 100 nm APS templates with europium of 0.54 and 1.35% mole, respectively. Scale bars in SEM and TEM images are 200 nm.

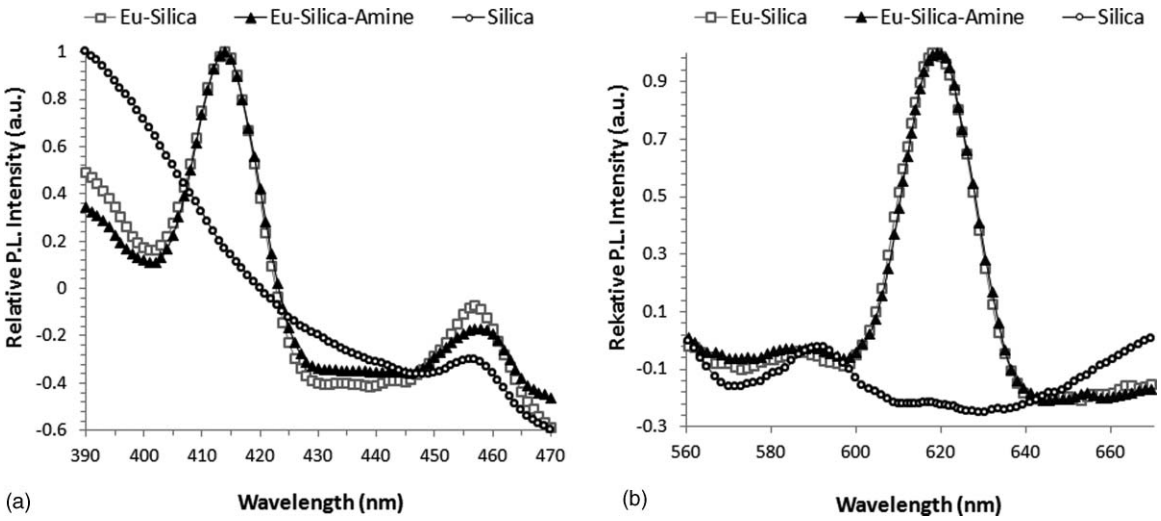

Fig. 2 (a) Excitation and (b) emission of 100 nm silica nanoshells, europium silica nanoshells (doped with 1.35% mole europium), and europium silica nanoshells surfaced functionalized with PEI.

liquid evaporates during the drying process.[22] In addition, X-ray diffraction analysis was performed on dry powdered NS samples and no crystalline material was observed (results not shown).

3.2 *Optical Properties*

Figure 2 shows the excitation (λem = 615 nm) and emission spectra of the 100 nm Eu-SiO_2 nanoshells containing 1.35 mole% Eu under 413 nm excitation. The $^5D_0$ emission of Eu^{3+} has five characteristic peaks, which are assigned to the $^5D_0$–^7F_J (J = 0, 1, 2, 3, 4) transitions. The strong emission centered at 615 nm can be attributed to the $^5D_0$–$^7F_2$ atomic like f-f transition.[23] Atomic emission lines dominate the luminescence of the Eu-SiO_2 and Eu-SiO_2-PEI particles, but it is not seen in the undoped SiO_2 nanoshells, signifying that the detected luminescence is due to the Eu incorporated on the NS surface.

3.3 *Dynamic Light Scattering and Zeta Potential Measurements*

Using DLS, the dispersed size of the Eu-SiO_2 nanoshells in aqueous suspension was estimated. All the concentrations of nanoshells in aqueous suspension were 3 mg/mL. After 3 h of sonication, 10 uL of suspension was diluted in 1 mL of de-ionized water for size and zeta potential determinations. Table 2 shows the sizes and zeta potentials of core-shell spheres (noncalcined silica coated APS spheres), NS, and PEI coated NS. The sizes measured in solution by DLS measurements are about double the sizes obtained from the SEM pictures. In the sol-gel reaction, growing colloidal silica could crosslink between spheres and form some dimers or trimers consistent with the core-shells having a larger diameter and polydispersity index (PDI) than their templates. TEM images show the shells of some spheres fused with neighboring shells, but it is difficult to quantify the amount of aggregation with TEM or SEM. Core-shell spheres possess a negatively charged surface from the silica gel coating the APS beads. After calcination, the amino-polystyrene core was removed, which resulted in the silica shell exhibiting an even more negative surface charge, perhaps due to the removal of the amino groups. The calcination also densified the silica shell and produced a smaller diameter and narrower size range. The small doping content of Eu^{3+} does not greatly affect the zeta potential of the NS.

Table 2 Size and zeta potential of silica nanoshells in aqueous suspension.[a]

	Average size (nm)	PDI	Zeta potential (mV)
Core-shell spheres	225	0.35	− 15
Nanoshells	157	0.22	− 22
PEI coated nanoshells	185	0.25	48

[a]Test is induced using 100-nm Eu-silica nanoshells with 1.35% mole europrium.

Particles with positively charged surfaces should enhance binding between particles and cells. Langer, etc.[24] reported that the zeta potential of PEI coated silica spheres could be up to + 47.90 mV. A 0.1% PEI aqueous solution was employed to coat the Eu-SiO_2 nanoshells. The pK_a of PEI in water is 9.6, so it is significantly protonated and readily absorbed to the negatively charged surface of Eu-SiO_2 nanoshells and trapped in the polar porous structure of SiO_2. A zeta potential of + 48 mV was observed for the NS after PEI coating. The zeta potential negative to positive charge change that occurred between the nonmodified NS (− 22 mV) and the PEI coated NS (+ 48 mV) imply the presence of amine groups on the PEI coated Eu-SiO_2 particle surface. The PEI coating only slightly increased the size of PEI modified NS compared to nonmodified ones.

3.4 *Adhesion/Endocytosis Experiments and Image Analysis*

In general, cell membranes tend to have a net negative charge due to surface glycoproteins/glycosphingolipids,[25] which has led many groups to take advantage of this unique cell property by functionalized short DNA sequences,[26] peptides,[27] proteins,[28]

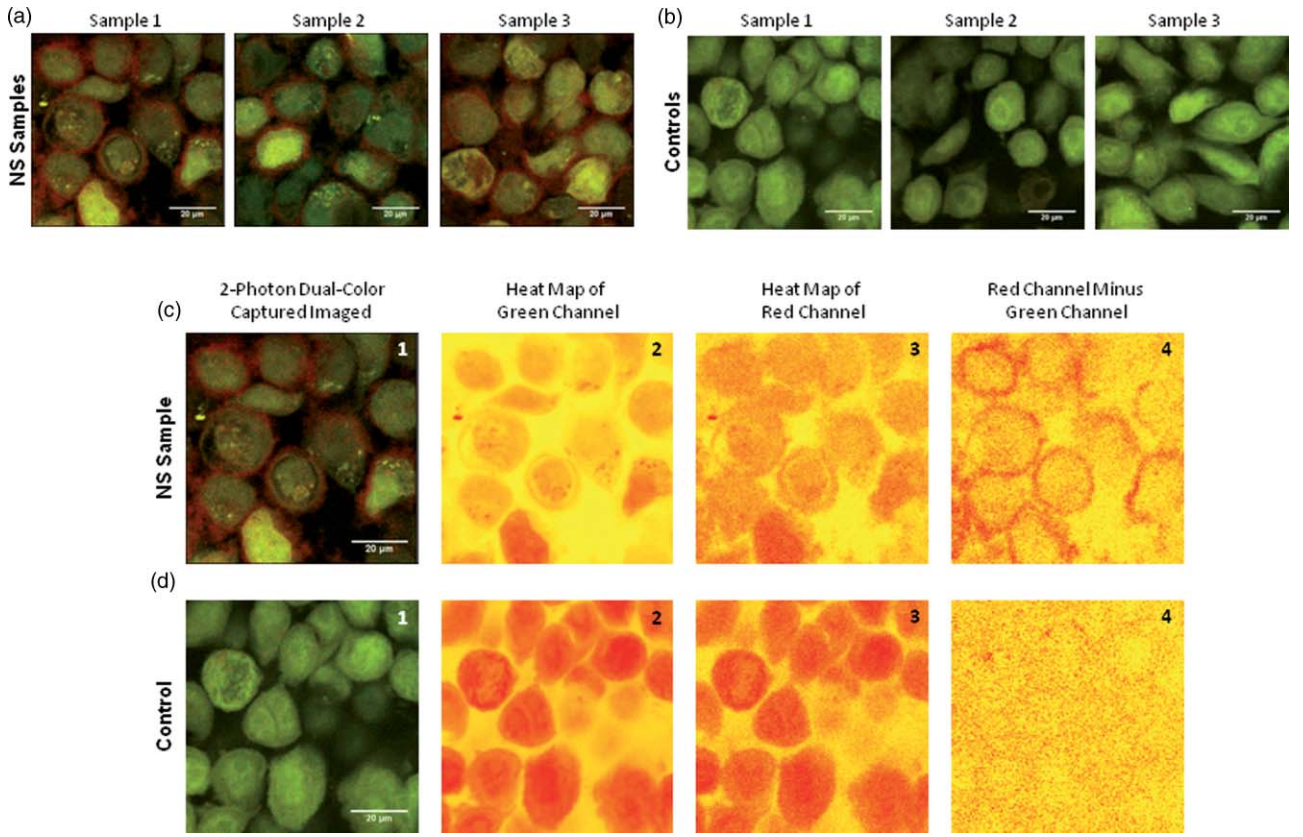

Fig. 3 Adhesion/endocytosis imaging of Eu-SiO_2 NS on HeLa cells. HeLa cells, stained with CMFDA (green), appear to have a red ring of NS around their cellular membrane when incubated with Eu-SiO_2-PEI NS (red) for 24 h [Panel (a)], while HeLa cell only controls do not [Panel (b)]. Results were confirmed by performing a background subtraction on samples incubated with [Panel (c)] and without [Panel (d)] Eu-SiO_2-PEI NS.

or NPs (Ref. 29) with cationic functional groups in order to help the macromolecules or nanoparticles adhere and penetrate mammalian cells through electrostatic mediated interactions. To implement this, the surface of the Eu-SiO_2 nanoshells was functionalized with PEI. In addition, the high positive charge on the NS surface due to the surface adsorbed PEI helps prevent the aggregation of the Eu-SiO_2 nanoshells under physiological conditions.[30]

The uptake of the Eu-SiO_2 NS coated with PEI was studied by two-photon (2-P microscopy) under *in vitro* cell culture conditions with HeLa cervical cancer cells. For these adhesion/endocytosis experiments Eu-SiO_2 NS with a DLS measured size of 332.7 nm (PDI: 0.202) and a zeta-potential 43.9 mV were used. As shown in Fig. 3(a), a high number of red emissive Eu-SiO_2 NS can be detected along the cell membrane of multiple HeLa cells when compared to control HeLa cells stained with CMFDA intercellular stain [Fig. 3(b)]. As the PEI coated particles carry a highly positive zeta potential (+ 48 mV, Table 1), electrostatic attraction of the particles to the negatively charged cell membrane could account for this observation.

In order to confirm that the red ring around the HeLa cells [Fig. 3(a)] was composed of Eu-SiO_2-PEI NS and not an optical artifact, a background subtraction between the red and green images was performed using custom C#-based heat map software. Briefly, optical bleed over from any green fluorescence passed through the red fluorescence filter could fasely indicate the prescence of Eu-doped NS particles. The recorded color fluorescent microscopy image was split into red, green, and blue channels and background subtraction was independently perfomed on each channel to remove baseline noise from the camera exposure. The intensity values of each pixel in the green fluorescence image were subtracted from each pixel in the red fluorescnence image (setting any negative values to zero), leaving only intensity values above and beyond any green fluorescence in the resultant image. The remaining intensity range of the image was then scaled across a red to yellow heat scale and averaged into 2×2 pixel blocks for visualization purposes. In summary, this subtraction removes any optical bleed from the green channel (CMFDA cytoplasmic stain) to the red channel (Eu-doped NS particles).

As shown in Figs. 3(c) and 3(d), the original 2-P dual-color image was first separated into its individual red and green channel components, and a multiple of the green channel heat map was subtracted from its red counterpart. These results clearly show that the samples incubated with PEI-NS have a ring of nanoparticles around the majority of the HeLa cells [Fig. 3(c)-4], but the control sample [Fig. 3(d)-4] does not have a similar feature, which is consistent with the PEI functionalized NS having attached to the surfaces of the HeLa cells.

A luminescence ratio analysis was performed on the outer and inner regions of the cell membrane in order to distinguish between the amount of PEI-NS attached to the outer part of the membrane and those internalized by the cells. To our knowledge, this is the first time a luminescence ratio analysis has been

Table 3 Emission ratio analysis results.

	Red mean luminescence / Green mean luminescence	Standard deviation
Controls: Outlines just outside of cell ($n = 25$)	0.80	0.087
NS samples: Outlines just outside of cell ($n = 33$)	2.58	0.57
Controls: Outlines inside of cell ($n = 25$)	0.80	0.03
NS samples: Outlines inside of cell ($n = 33$)	1.07	0.17

used to demonstrate the adhesion/endocytosis of NPs onto cells. This was accomplished by using Image J to create outline areas just outside or inside the cell, based on the green cytoplasmic cell stain images on both the control and PEI-NS sample images; apply these same outlines to their corresponding locations on the red channel image using the ROI manager; and use the analyze particles/measure tools to calculate the mean luminescence values of the outline areas, in both the green and red channels. Once the mean luminescent value of each outline area was known, the ratio of red to green mean luminescence ratio was calculated for each outline.

The ratio analysis performed on the outlines just outside of the cell samples incubated with Eu-SiO_2-PEI NS had a luminescence ratio of 2.58 (SD $\pm$ 0.57) (Table 3), while the control samples had a ratio of 0.80 ($\pm$ 0.09); therefore, the samples with europium-SiO_2-PEI NS are $\sim$223% more photoluminescently intense in areas around the periphery of HeLa cells than native HeLa cells. These results imply that a large number of Eu-SiO_2-PEI NS are attached to the outer membrane surface of the HeLa cells, which is consistent with the expected electrostatic attraction of the positively charged particles to the negatively charged cell membrane. Conversely, when the ratio analysis was performed on areas located inside the cell [Figs. 4(a)-5/4(a)-4 and 4(b)-5/4(b)-4], it was found that the Eu-SiO_2-PEI NS samples were only $\sim$ 34% more luminescently intense (Table 3), which is consistent with a small amount of Eu-SiO_2-PEI NS penetrating the cell membrane by endocytosis. It is hypothesized that the negligible amount of endocytosis is probably due to the lack of targeting to a specific membrane receptor.

Previous studies by Oh and colleagues[31] have proposed that optimal nanoparticle uptake into cells typically occurs with particles between the range of 50 to 200 nm, while other groups have shown that sub-100 nm particles exhibit significantly greater cellular uptake compared with particles >100 nm diameter regardless of the surface composition of the particles.[32–34] Therefore, it is proposed that improved NS cellular uptake could be induced

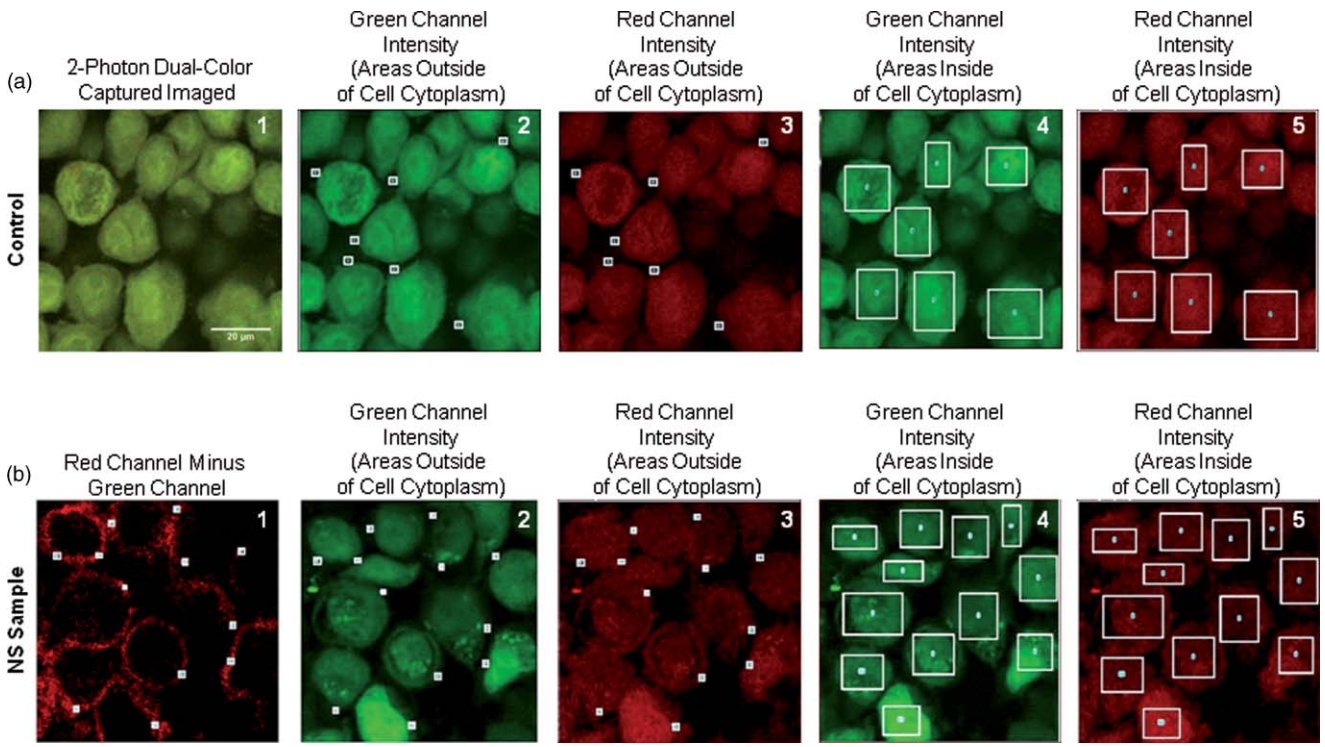

Fig. 4 Fluorescent intensity ratio analysis of adhesion/endocytosis experiments. Panel (a), shows outline areas just outside [(a)-2 and (a)-3] or inside [(a)-4 and (a)-5] HeLa cells for a typical control sample, while Panel (b), shows similar outlines for cells incubated with Eu-SiO_2-PEI NS. Outlines on individual images that were used to determine the red to green mean luminescence ratios for each sample set are shown. The average emission intensity ratio of areas just outside the cell membrane wall was typically 223% more luminescently intense for samples incubated with Eu-SiO_2-PEI NS, when compared to HeLa cells controls stained only with CMFDA. All outlines were based on the location of the green cytoplasmic cell stain images.

by reducing the size of the NS. In addition to size consideration, particle uptake can be enhanced by functionalizing the surface of the NS with a targeting ligand that can bind to specific cell surface receptors that can induce endosomal endocytosis. For example, previous work by Rosenholm, etc.[30] has shown that folate targeted nanoparticles tend to be readily endocytosed by HeLa cells, even when the nanoparticle diameter is larger than 400 nm.

4 Conclusions

Photoluminescent Eu^{3+} has been doped into 100 and 200 nm diameter sizes of silica NS through a sol-gel synthesis route and use of a polymer bead template. Removing the polymer cores by calcination produces silica NS containing less than 3% mole europium, which emits a strong narrow red emission line at 615 nm. The long lifetime of the rare earth ion facilitates studies by 2-P microscopy. Two-photon microscopy of the europrium (III) doped NS show little interaction with HeLa cells in culture media; however, when the NS were coated with PEI they acquired a high positive charge and bound to the outer surface of HeLa cancer cells with minimal endocytosis. The ability to control nanoparticle location (cell surface versus interior) is valuable in biosensing and drug delivery studies.

Acknowledgments

This research was supported by NIH Nanotumor (Grant No. U54 CA 119335) and we thank the California Institute of Information Technology and Telecommunication for research support. In addition, individual student funding was provided by NCI Research Supplements to Promote Diversity in Health Related Research Fellowship (NIH Grant No. 3U54 CA 119335–05S3), NSF—California LSAMP Bridge to the Doctorate/Louis Stokes Alliances for Minority Participation Fellowship (UCI NSF Grant No. HRD0115115), and NIH—ET CURE/Specialized Cancer Center Support (Grant No. 3P30 CA 023100–25S7). The NIH National Center for Microscopy and Imaging Research at UCSD is acknowledged for assistance with obtaining the TEM images.

References

1. C. Barbe, J. Bartlett, L. G. Kong, K. Finnie, H. Q. Lin, M. Larkin, S. Calleja, A. Bush, and G. Calleja, "Silica particles: a novel drug-delivery system," *Adv. Mater.* **16**(21), 1959–1966 (2004).
2. P. Sharrna, S. Brown, G. Walter, S. Santra, and B. Moudgil, "Nanoparticles for bioimaging," *Adv. Colloid Interface Sci.* **123**, 471–485 (2006).
3. C. W. Lai, J. K. Hsiao, Y. C. Chen, and P. T. Chou, *Nanomaterials for the Life Sciences*, vol. 3, Wiley, New York (2009).
4. Y. Jin, S. Lohstreter, and J. X. Zhao, *Nanomaterials for the Life Sciences*, vol. 2, Wiley, New York (2009).
5. A. M. Lipski, C. Jaquiery, H. Choi, D. Eberli, M. Stevens, I. Martin, I. W. Chen, and V. P. Shastri, "Nanoscale engineering of biomaterial surfaces," *Adv. Mater.* **19**(4), 553–557 (2007).
6. J. E. Smith, L. Wang, and W. T. Tan, "Bioconjugated silica-coated nanoparticles for bioseparation and bioanalysis," *TrAC, Trends Anal. Chem.* **25**(9), 848–855 (2006).
7. H. Choi and I. W. Chen, "Surface-modified silica colloid for diagnostic imaging," *J. Colloid Interface Sci.* **258**(2), 435–437 (2003).
8. T. K. Jain, I. Roy, T. K. De, and A. Maitra, "Nanometer silica particles encapsulating active compounds: a novel ceramic drug carrier," *J. Am. Chem. Soc.* **120**(43), 11092–11095 (1998).
9. J. Kim, J. E. Lee, J. Lee, J. H. Yu, B. C. Kim, K. An, Y. Hwang, C. H. Shin, J. G. Park, J. Kim, and T. Hyeon, "Magnetic fluorescent delivery vehicle using uniform mesoporous silica spheres embedded with monodisperse magnetic and semiconductor nanocrystals," *J. Am. Chem. Soc.* **128**(3), 688–689 (2006).
10. D. J. Bharali, I. Klejbor, E. K. Stachowiak, P. Dutta, I. Roy, N. Kaur, E. J. Bergey, P. N. Prasad, and M. K. Stachowiak, "Organically modified silica nanoparticles: a nonviral vector for in vivo gene delivery and expression in the brain," *Proc. Natl. Acad. Sci. U.S.A.* **102**(32), 11539–11544 (2005).
11. F. Torney, B. G. Trewyn, V. S. Y. Lin, and K. Wang, "Mesoporous silica nanoparticles deliver DNA and chemicals into plants," *Nat. Nanotechnol.* **2**(5), 295–300 (2007).
12. W. H. Tan, K. M. Wang, X. X. He, X. J. Zhao, T. Drake, L. Wang, and R. P. Bagwe, "Bionanotechnology based on silica nanoparticles," *Med. Res. Rev.* **24**(5), 621–638 (2004).
13. A. Burns, H. Ow, and U. Wiesner, "Fluorescent core-shell silica nanoparticles: towards 'Lab on a Particle' architectures for nanobiotechnology," *Chem. Soc. Rev.* **35**(11), 1028–1042 (2006).
14. D. Knopp, D. P. Tang, and R. Niessner, "Bioanalytical applications of biomolecule-functionalized nanometer-sized doped silica particles," *Anal. Chim. Acta* **647**(1), 14–30 (2009).
15. V. Cauda, A. Schlossbauer, J. Kecht, A. Zurner, and T. Bein, "Multiple core-shell functionalized colloidal mesoporous silica nanoparticles," *J. Am. Chem. Soc.* **131**(32), 11361–11370 (2009).
16. M. C. Estevez, M. B. O'Donoghue, X. L. Chen, and W. H. Tan, "Highly fluorescent dye-doped silica nanoparticles increase flow cytometry sensitivity for cancer cell monitoring," *Nano Res.* **2**(6), 448–461 (2009).
17. Y. Xu, A. Karmakar, D. Y. Wang, M. W. Mahmood, F. Watanabe, Y. B. Zhang, A. Fejleh, P. Fejleh, Z. R. Li, G. Kannarpady, S. Ali, A. R. Biris, and A. S. Biris, "Multifunctional Fe3O4 cored magnetic-quantum dot fluorescent nanocomposites for RF nanohyperthermia of cancer cells," *J. Phys. Chem. C* **114**(11), 5020–5026 (2010).
18. Y. T. Lim, J. K. Kim, Y. W. Noh, M. Y. Cho, and B. H. Chung, "Multifunctional silica nanocapsule with a single surface hole," *Small* **5**(3), 324–328 (2009).
19. L. Y. Chen, C. L. Chen, R. N. Li, Y. Li, and S. Q. Liu, "CdTe quantum dot functionalized silica nanosphere labels for ultrasensitive detection of biomarker," *Chem. Commun. (Cambridge)* **19**, 2670–2672 (2009).
20. T. Andelman, S. Gordonov, G. Busto, P. Moghe, and R. Riman, "Synthesis and cytotoxicity of Y2O3 nanoparticles of various morphologies," *Nanoscale Res. Lett.* **5**(2), 263–273 (2010).
21. J. Yang, J. U. Lind, and W. C. Trogler, "Synthesis of hollow silica and titania nanospheres," *Chem. Mater.* **20**(9), 2875–2877 (2008).
22. C. J. Brinker and G. W. Scherer, *Sol-gel Science: The Physics and Chemistry of Sol-Gel Processing*, pp. 9–10, Academic, New York (1990).
23. M. H. V. Werts, "Making sense of lanthanide luminescence," *Sci. Prog.* **88**, 101–131 (2005).
24. J. E. Fuller, G. T. Zugates, L. S. Ferreira, H. S. Ow, N. N. Nguyen, U. B. Wiesner, and R. S. Langer, "Intracellular delivery of core-shell fluorescent silica nanoparticles," *Biomaterials* **29**(10), 1526–1532 (2008).
25. N. R. Yacobi, N. Malmstadt, F. Fazlollahi, L. DeMaio, R. Marchelletta, S. F. Hamm-Alvarez, Z. Borok, K. J. Kim, and E. D. Crandall, "Mechanisms of alveolar epithelial translocation of a defined population of nanoparticles," *Am. J. Respir. Cell Mol. Biol.* **42**(5), 604–614 (2010).
26. A. Schroeder, C. G. Levins, C. Cortez, R. Langer, and D. G. Anderson, "Lipid-based nanotherapeutics for siRNA delivery," *J. Intern. Med.* **267**(1), 9–21 (2010).
27. D. S. Daniels and A. Schepartz, "Intrinsically cell-permeable miniature proteins based on a minimal cationic PPII motif," *J. Am. Chem. Soc.* **129**(47), 14578–14579 (2007).
28. A. D. Frankel and C. O. Pabo, "Cellular uptake of the tat protein from human immunodeficiency virus," *Cell* **55**(6), 1189–1193 (1988).
29. S. Hong, A. U. Bielinska, A. Mecke, B. Keszler, J. L. Beals, X. Shi, L. Balogh, B. G. Orr, J. R. Baker, Jr., and M. M. Banaszak Holl, "Interaction of poly(amidoamine) dendrimers with supported lipid bilayers and cells: hole formation and the relation to transport," *Bioconjugate Chem.* **15**(4), 774–782 (2004).
30. J. M. Rosenholm, A. Meinander, E. Peuhu, R. Niemi, J. E. Eriksson, C. Sahlgren, and M. Linden, "Targeting of porous hybrid silica nanoparticles to cancer cells," *ACS Nano* **3**(1), 197–206 (2009).

31. J. M. Oh, S. J. Choi, G. E. Lee, J. E. Kim, and J. H. Choy, "Inorganic metal hydroxide nanoparticles for targeted cellular uptake through clathrin-mediated endocytosis," *Asian J. Chem.* **4**(1), 67–73 (2009).
32. I. Slowing, B. G. Trewyn, and V. S. Lin, "Effect of surface functionalization of MCM-41-type mesoporous silica nanoparticles on the endocytosis by human cancer cells," *J. Am. Chem. Soc.* **128**(46), 14792–14793 (2006).
33. M. P. Desai, V. Labhasetwar, E. Walter, R. J. Levy, and G. L. Amidon, "The mechanism of uptake of biodegradable microparticles in Caco-2 cells is size dependent," *Pharm. Res.* **14**(11), 1568–1573 (1997).
34. S. Prabha, W. Z. Zhou, J. Panyam, and V. Labhasetwar, "Size-dependency of nanoparticle-mediated gene transfection: studies with fractionated nanoparticles," *Int. J. Pharm.* **244**(1–2), 105–115 (2002).